PHYSICAL REVIEW D VOLUME 24, NUMBER 3 1 AUGUST 1981

Quark-bag model with low-energy pion interactions. II. Application

C. E. DeTar
Department of Physics, University of Utah, Salt Lake City, Utah 84112
(Received 12 November 1980)

The hybrid pion–quark-bag model discussed in I is applied to a calculation of masses, pion couplings, and other parameters of various light hadrons in an effort to determine the extent to which the bag parameters must be modified in the presence of pion interactions. Corrections for the finite spread of the c.m. wave packet are also included in each case.

I. INTRODUCTION

In order to apply the hybrid chiral models, discussed in Ref. 1 (I), to such interesting processes as the two-nucleon interaction, it is necessary to determine the extent to which coupling to the pion requires changes in the parameters of the bag model.[2,3] Although others studied these changes[4-6] none has considered obtaining agreement with a large assortment of static parameters and masses at the same time except the authors of Ref. 7. In addition important corrections for the bag c.m. motion have not been included.[8,9]

Our perturbative analysis begins with the modified action of I and Ref. 6 written here to first order in $1/f$, the inverse pion decay constant:

$$A=\int_V d^4x\left(\frac{i}{2}\bar{q}\gamma\cdot\partial q-B\right)-\int d^4x\,\tfrac{1}{2}(\partial_\mu\vec{\pi})^2+A_1\,,$$
$$A_1=-\tfrac{1}{2}\int_S d^3x\,\bar{q}(1+i\vec{\tau}\cdot\vec{\pi}\gamma_5/f)q\,. \tag{1.1}$$

Since the pion field extends continuously into the bag, a plane-wave basis is suitable for perturbation theory.

Starting with the modified action (1.1) we proceed to calculate to order $1/f^2$ in pion perturbation theory and in the static approximation (no nucleon recoil) the magnetic moments and charge radii of the nucleons, the axial-vector coupling constant of the nucleon, and the decay width of the Δ. To facilitate the calculation we derive Feynman rules for the various couplings to the static bag in Sec. II. The parameters listed above depend directly on the radius of the nucleon and the c.m. kinetic energy but not explicitly on other parameters such as the color coupling constant and bag constant. They are calculated and adjusted for the motion of the c.m. wave function in Sec. III. Results are presented as a function of the bag radius in Fig. 4. In Sec. IV we describe and present results of a calculation of the mass renormalization of the nucleon and $\Delta(1232)$, and the ρ, ω, and π mesons. Conclusions are given in Sec. V.

II. FEYNMAN RULES FOR PION-BAG COUPLING

To facilitate perturbative calculations of the renormalization of various parameters we use the Feynman rules listed in Figs. 1 and 2. Their derivation is sketched here.

The static-cavity approximation requires the neglect of baryon recoil[10]; hence the use of static propagators for the nucleon and Δ. The spin degree of freedom for the Δ is written in tensor notation so that the spinor $U_{\nu j}$ satisfies

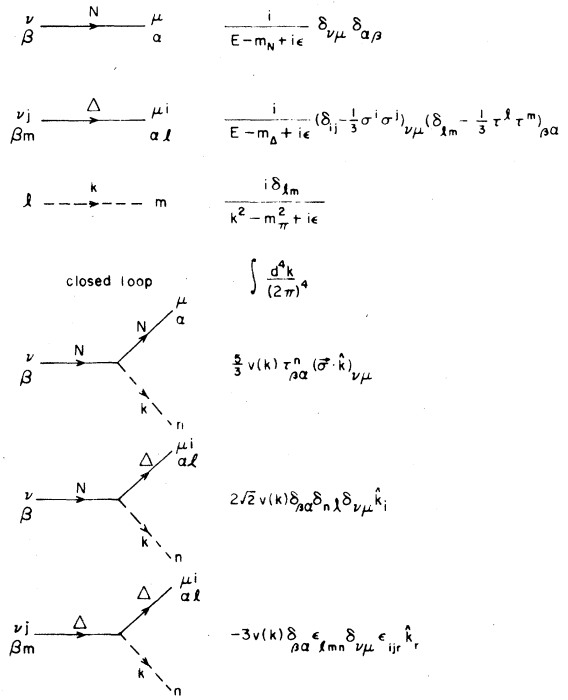

FIG. 1. Feynman rules in the static limit, derived from pion-bag coupling. A $\frac{1}{2}\otimes 1$ basis is used for spin $\frac{3}{2}$ and isospin $\frac{3}{2}$. The indices μ,ν,i,j and the spinor σ refer to spin and α, β, l, m and the spinor τ isospin. The form factor $v(k)$ is given by (2.4) with appropriate choice of R.

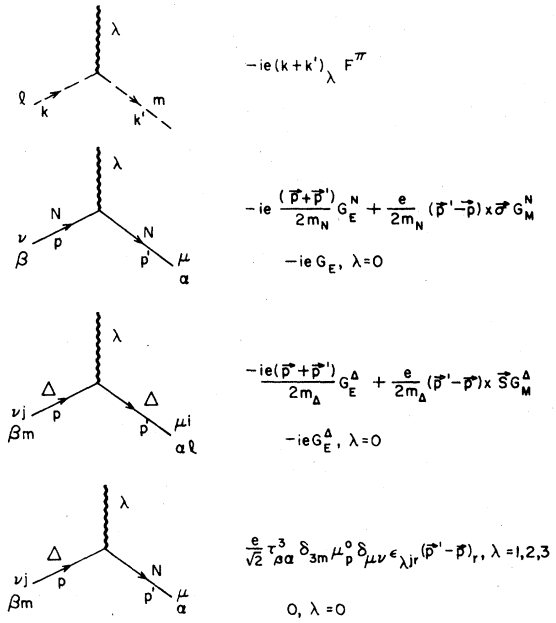

FIG. 2. The corresponding rules for electromagnetic coupling. To low order in $q^2=(\vec{p}'-\vec{p})^2$ the bare bag form factors are

$$F^\pi=-i\epsilon_{lm3}(1-\tfrac{1}{6}\langle r_\pi^2\rangle q^2),$$
$$G_E^N=\delta_{\mu\nu}(\tfrac{1}{2}+\tfrac{1}{2}\tau^3)_{\beta\alpha}(1-\tfrac{1}{6}\langle r_p^2\rangle_0 q^2),$$
$$G_E^\Delta=\delta_{\mu\nu}Q_{\beta m,\alpha l}(1-\tfrac{1}{6}\langle r_p^2\rangle_0 q^2),$$
$$G_M^N=\delta_{\mu\nu}(\tfrac{1}{6}+\tfrac{5}{6}\tau_3)_{\beta\alpha}2m_N\mu_p^0,$$

and

$$G_M^\Delta=\tfrac{2}{3}Q_{\beta m,\alpha l}2m_\Delta\mu_p^0,$$

the spin-$\frac{3}{2}$ operator is $S_r=\frac{1}{2}\sigma^r_{\mu\nu}\delta_{ij}-i\delta_{\mu\nu}\epsilon_{jir}$, and charge, $Q_{\beta m,\alpha l}=\frac{1}{2}\tau_{\beta\alpha}\delta_{ml}-i\delta_{\beta\alpha}\epsilon_{ml3}+\frac{1}{2}$.

$$\sum_{\nu=-1/2}^{1/2}\sum_{j=1}^{3}\sigma^j_{\mu\nu}U^m_{\nu j}=0 \tag{2.1}$$

and

$$\sum_{m=-3/2}^{3/2}U^{m*}_{\nu j}U^m_{\mu k}=P_{3/2}=(\delta_{jk}-\tfrac{1}{3}\sigma^j\sigma^k)_{\mu\nu}\,. \tag{2.2}$$

The baryon couplings are obtained by calculating the matrix elements of iA_1 between the various bag and bag-pion states. Thus, for example,

$$\langle\vec{\pi}(\vec{k})N'|iA_1|N\rangle=\frac{2\pi i\delta(E-E'-\omega(k))}{(2\omega(k))^{1/2}(2\pi)^{3/2}}\frac{5}{3}\vec{\sigma}\cdot\hat{k}\vec{\tau}\tilde{v}(kR)\,, \tag{2.3}$$

where

$$\tilde{v}(kR)=\tfrac{9}{10}g_A^0 j_1(kR)/fR\,, \tag{2.4}$$

and

$$g_A^0=\frac{5}{9}\frac{x}{x-1} \tag{2.5}$$

is the bare nucleon axial-vector charge.[1] Since $x\approx 2.04$ for the $S_{1/2}$-cavity eigenmode, $g_A^0=1.09$. The operators σ and $\vec{\tau}$ act on the nucleon spinors. In (2.3) the quark wave functions are taken to be unperturbed by gluon interactions.

A similar analysis yields the basic $\pi N\Delta$ and $\pi\Delta\Delta$ couplings listed in Fig. 1. The bare πNN coupling constant is given, of course, by the Goldberger-Treiman relation:

$$g_0=\frac{g_A^0 m_N}{f}\,. \tag{2.6}$$

The renormalized constants also satisfy this relation within our approximation of neglecting variations in form factors due to the continuation to physical masses. The bare width of the $\Delta(1232)$ is given by[11]

$$\Gamma_\Delta^0=\frac{4}{3\pi}v^2(k_\Delta R_\Delta)k_\Delta\,, \tag{2.7}$$

where $k_\Delta=227$ MeV, the physical-pion c.m. momentum. No recoil correction has been made. Each vertex is proportional to the same form factor (2.4), since the calculation is carried out in the SU(6) limit, neglecting gluon interactions. However, in application it is intended that the baryon legs be evaluated for physical masses. The nucleon and Δ have slightly different radii when gluon interactions are considered, so we have used R_N when renormalizing the nucleon mass and R_Δ for the Δ.[12] In any case, for small k the form factor is quite insensitive to R. It will be observed that $j_1(kR)$ oscillates for large k because of the sharp bag boundary. In this region the pointlike-field approximation for the pion is not valid, nor is the sharp boundary realistic. Therefore we introduce a cutoff at the first zero of j_1 where $kR\approx 4.5$. We have then

$$v(kR)=\tilde{v}(kR)\theta(4.5-kR)\,. \tag{2.8}$$

This aesthetic cutoff is not necessary to provide convergence of self-energies, etc., as in the original cutoff static pion-nucleon field theories.[13] Convergence is inherent in the behavior of the Bessel function. Removing the cutoff changes self-energies by only a few percent.

For completeness the electromagnetic form factors for the "bare" nucleon, "bare" Δ, and π have been included in Fig. 2. Again these quantities are calculated in the no-recoil approximation.[2] Hence, only the low-frequency behavior is plausible—i.e., the static magnetic moments and the charge radii. To some extent it is possible to correct for the neglect of recoil when the c.m. wave packet is taken into account. However, in the absence of a detailed knowledge of the c.m. wave function, higher moments cannot be calcula-

ted reliably. Thus

$$G_E(q^2)=\left\langle N\left|:\int q^\dagger(r)q(r)e^{i\vec{q}\cdot\vec{r}}d^3r:\right|N\right\rangle = 1-\tfrac{1}{6}\langle r^2\rangle q^2,$$
$$G_M(0)=\left\langle N\left|:\int \tfrac{1}{2}\vec{r}\times q^\dagger(r)\vec{\alpha}q(r)\,d^3r:\right|N\right\rangle = \frac{R}{12}\frac{4x-3}{x(x-1)}, \tag{2.9}$$

where in the approximation of neglecting gluon and pion interactions

$$\langle r_n^2\rangle_0=0\,,\quad \langle r_p^2\rangle_0=-0.530R^2$$

and

$$\mu_p^0=0.202R\,,\quad \mu_n^0/\mu_p^0=-\tfrac{2}{3}\,.$$

The pion is given its physical charge radius of $\langle r_\pi^2\rangle^{1/2}=0.78$.[14]

III. RENORMALIZATION OF STATIC NUCLEON PARAMETERS

We give here results of a calculation of the nucleon magnetic moments, charge radii, the nucleon axial-vector charge, and the decay width of the Δ. The bare quantities are corrected for pion interactions to order $1/f^2$. In computing the corrections we have used throughout the values $g_A=1.24$ and $f=93$ MeV in $v(kR)$ in the highest-order term as a matter of convenience. The difference between values obtained with this choice and the use of the unrenormalized value is of the same size as the neglected higher-order terms in $1/f^2$, and so is no greater than the expected error. The correction for the finite spread of the c.m. wave packet is applied to the bare quantities. No attempt has been made to correct the pion renormalized quantities for the c.m. motion—i.e., the c.m. correction and pion correction are both treated independently as though they were of the same order. The quantitative justification for this treatment is given in the discussion (Subsection F) below.

A. Wave-function renormalization

The single-loop pion self-energy for the nucleon and Δ [Fig. 3(a)] is

$$\Sigma_N(E)=\frac{25}{3}\frac{1}{(2\pi)^2}\int_{m_\pi}^\infty \frac{k\,d\omega\,v^2(kR_N)}{(E-\omega-m_N+i\epsilon)} + \frac{32}{3}\frac{1}{(2\pi)^2}\int_{m_\pi}^\infty \frac{k\,d\omega\,v^2(kR_N)}{(E-\omega-m_\Delta+i\epsilon)}, \tag{3.1}$$

$$\Sigma_\Delta(E)=\frac{8}{3}\frac{1}{(2\pi)^2}\int_{m_\pi}^\infty \frac{k\,d\omega\,v^2(kR_\Delta)}{(E-\omega-m_N+i\epsilon)} + \frac{25}{3}\frac{1}{(2\pi)^2}\int_{m_\pi}^\infty \frac{k\,d\omega\,v^2(kR_\Delta)}{(E-\omega-m_\Delta+i\epsilon)},$$

where $\omega=(k^2+m_\pi^2)^{1/2}$. To this order the masses m_N and m_Δ are taken to be the real parts of the physical masses and $v(kR)$ in (2.4) and (2.8) is defined in terms of the renormalized constants $g_A=1.24$ and $f=93$ MeV. The mass shifts are given by

$$\delta m_N=\Sigma_N(m_N)\,,\quad \delta m_\Delta=\Sigma_\Delta(m_\Delta)\,, \tag{3.2}$$

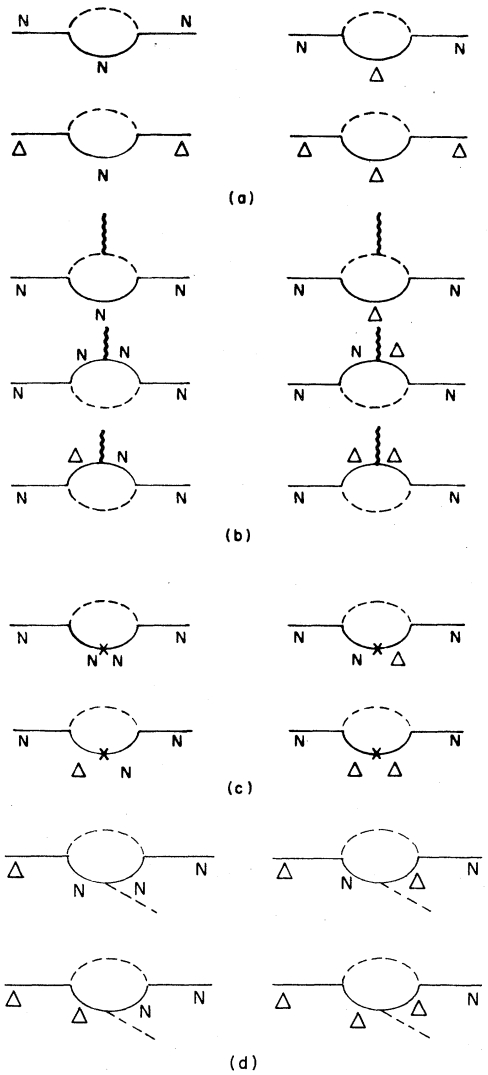

FIG. 3. Diagrams contributing to (a) baryon self-energy to order $1/f^2$, (b) electromagnetic vertex renormalization, (c) nucleon axial-vector-current renormalization, (d) $\pi N\Delta$ coupling-constant renormalization.

and the wave-function renormalization factors are given by

$$Z_N = 1 - \epsilon_N\,, \quad Z_\Delta = 1 - \epsilon_\Delta\,, \tag{3.3}$$

where

$$\epsilon_N = -\Sigma_N'(m_N) = \frac{25}{3}\frac{1}{(2\pi)^2}\int_{m_\pi}^{\infty}\frac{k\,d\omega\,v^2(kR_N)}{\omega^2} + \frac{32}{3}\frac{1}{(2\pi)^2}\int_{m_\pi}^{\infty}\frac{k\,d\omega\,v^2(kR_N)}{(\omega_\Delta+\omega)^2}\,, \tag{3.4a}$$

$$\epsilon_\Delta = -\,\mathrm{Re}\,\Sigma_\Delta'(m_\Delta) = \frac{-d}{dE}\frac{8}{3}\frac{1}{(2\pi)^2}\mathrm{P}\int_{m_\pi}^{\infty}\frac{k\,d\omega\,v^2(kR_\Delta)}{(E-\omega-m_N)}\Big|_{E=m_\Delta} + \frac{25}{3}\frac{1}{(2\pi)^2}\int_{m_\pi}^{\infty}\frac{k\,d\omega\,v^2(kR_\Delta)}{\omega^2}\,, \tag{3.4b}$$

and $\omega_\Delta = m_\Delta - m_N$.

The factors $Z_N^{1/2}$ and $Z_\Delta^{1/2}$ multiply each vertex with an external nucleon and Δ line, respectively. Since Z_N and Z_Δ are both less than 1, they reduce the bare values.

B. Nucleon magnetic moment

The wave-function renormalization contributes to the bare moments

$$\delta\mu_Z = -(\tfrac{1}{6}+\tfrac{5}{6}\tau_3)\mu_p^0\epsilon_N\,. \tag{3.5}$$

Four vertex corrections shown in Fig. 3(b) also contribute to the magnetic moment. The contribution from the pion current is

$$\delta\mu_\pi = \tau_3\left[\frac{100}{27}\frac{1}{(2\pi)^2}\int\frac{k\,d\omega\,v^2(kR_N)}{\omega^3} + \frac{32}{27}\frac{1}{(2\pi)^2}\int\frac{k\,d\omega\,v^2(kR_N)(\omega_\Delta+2\omega)}{2\omega^2(\omega+\omega_\Delta)^2}\right]. \tag{3.6}$$

The nucleon and Δ vertex corrections are

$$\delta\mu_N = -\tfrac{25}{9}(\tfrac{1}{2}-\tfrac{5}{6}\tau_3)\mu_p^0\frac{1}{(2\pi)^2}\int\frac{k\,d\omega\,v^2(kR_N)}{\omega^2}\,, \qquad \delta\mu_\Delta = \tfrac{80}{27}(1+\tfrac{5}{3}\tau_3)\mu_p^0\frac{1}{(2\pi)^2}\int\frac{k\,d\omega\,v^2(kR_N)}{(\omega+\omega_\Delta)^2}\,. \tag{3.7}$$

Finally the correction for the motion of the c.m. is made to the bare vertex. Following Donoghue and Johnson[8] we write

$$|N,\mathrm{bag}\rangle = \int d^3p\,\phi(p)|N,\vec{p}\rangle\,, \tag{3.8}$$

where $\phi(p)$ is the momentum-space wave function, normalized according to

$$\int d^3p\,|\phi(p)|^2 = 1\,. \tag{3.9}$$

Then

$$\int d^3x\,e^{i\vec{q}\cdot\vec{x}}\langle N_2,\mathrm{bag}|J^\mu(\vec{x},0)|N_1,\mathrm{bag}\rangle = \int d^3p\,\phi^*(\vec{p}+\vec{q}/2)\phi(\vec{p}-\vec{q}/2)\frac{m^2}{(E_2E_1)^{1/2}} \times\bar{U}_2[F_1(q^2)\gamma^\mu + F_2(q^2)iq_\nu\sigma^{\mu\nu}/2m]U_1\,, \tag{3.10}$$

where $E_2 = E(\vec{p}-\vec{q}/2)$ and $E_1 = E(\vec{p}+\vec{q}/2)$ and U_1 and U_2 are plane-wave spinors for the nucleons.[15] The matrix element on the left-hand side is calculated in the static cavity approximation, leading to (2.9) for the uncorrected electromagnetic form factors. The three-vector matrix element on the right-hand side gives, for small q,

$$\frac{i\vec{q}\times\vec{\sigma}}{2m}\,4\pi\int p^2dp\,|\phi(p)|^2\left[\left(1-\frac{2}{3}\frac{p^2}{m^2}+\frac{7}{12}\frac{p^4}{m^4}\right)Q + (2m\mu-Q)\left(1-\frac{p^2}{6m^2}+\frac{p^4}{8m^4}\right) + O(p^6/m^6)\right], \tag{3.11}$$

where μ is the corrected magnetic moment and Q is the nucleon charge in units of e. Thus the c.m. correction yields

$$2m\delta\mu_{\mathrm{c.m.}} = \left(\frac{1}{2}+\frac{\tau_3}{2}\right)\left(\frac{\langle p^2\rangle}{2m^2}-\frac{3}{8}\frac{\langle p^4\rangle}{m^4}\right) + \left(\frac{1}{6}\frac{\langle p^2\rangle}{m^2}-\frac{1}{8}\frac{\langle p^4\rangle}{m^4}\right)2m\mu_p^0(\tfrac{1}{6}+\tfrac{5}{6}\tau_3)\,. \tag{3.12}$$

Following Johnson[2] we estimate

$$\langle p^2\rangle = 3(\bar{x}/R)^2\,, \tag{3.13}$$

with $\bar{x} = 2.04$ in the present calculation, and we drop the terms in $\langle p^4\rangle/m^4$. The pion corrections are calculated using the physical values for g_A in $v(kR)$ here and throughout.

The corrected magnetic moments for the neutron and proton are displayed in Fig. 4 as a function of R_N. In Table I the various contributions are summarized.

C. Nucleon charge radius

The wave-function renormalization contributes to the bare value (2.6)

$$\delta\langle r^2\rangle_Z = -\langle r^2\rangle_0(\tfrac{1}{2}+\tfrac{1}{2}\tau_3)\epsilon_N\,. \tag{3.14}$$

The four vertex corrections of Fig. 3(b) are, respectively, these:

$$\delta\langle r^2\rangle_\pi = \tau_3\frac{50}{9}\frac{1}{(2\pi)^2}\int\frac{k\,d\omega\,v^2(kR_N)}{\omega^2}\left(\langle r_\pi^2\rangle+\frac{2}{k^2}+\frac{9}{4\omega^2}-\frac{5}{4}\frac{k}{\omega^4}+D\right) - \tau_3\frac{32}{9}\frac{1}{(2\pi)^2}\int\frac{k\,d\omega\,v^2(kR_N)}{(\omega_\Delta+\omega)^2}\left[\langle r_\pi^2\rangle+\frac{2}{k^2}+\frac{3}{4\omega^4}+\frac{3}{2\omega(\omega_\Delta+\omega)_\Delta}-\frac{k^2}{2\omega^3(\omega_\Delta+\omega)}-\frac{k^2}{2\omega^2(\omega_\Delta+\omega)^2}+D\right], \tag{3.15}$$

TABLE I. Proton and neutron magnetic moments, proton and neutron charge radii (in fm), nucleon axial-vector charge, and decay width of Δ, as modified by pion interactions to order $1/f^2$ and the c.m. motion, for various nucleon bag radii.

$R_N(\mathrm{GeV}^{-1})$	3.5	4.0	4.5	5.0	5.5	6.0	6.5	7.0
proton								
$2m\delta\mu_Z$	−0.97	−0.79	−0.66	−0.56	−0.48	−0.41	−0.36	−0.31
$2m\delta\mu_{N,\Delta}$	0.32	0.25	0.20	0.17	0.14	0.11	0.10	0.09
$2m\delta\mu_\pi$	0.96	0.77	0.62	0.51	0.43	0.36	0.31	0.27
$2m(\delta\mu_Z+\delta\mu_{N,\Delta}+\delta\mu_\pi)$	0.31	0.23	0.17	0.13	0.10	0.07	0.05	0.04
$2m\delta\mu_{\mathrm{c.m.}}$	0.84	0.67	0.55	0.75	0.63	0.54	0.47	0.42
$2m\mu_0$	1.33	1.52	1.71	1.90	2.09	2.28	2.47	2.66
$2m_\mu$	2.47	2.41	2.43	2.49	2.82	2.89	2.99	3.11
neutron								
$2m\delta\mu_Z$	0.65	0.53	0.44	0.37	0.31	0.27	0.23	0.20
$2m\delta\mu_{N,\Delta}$	−0.34	−0.29	−0.24	−0.20	−0.18	−0.15	−0.13	−0.11
$2m\delta\mu_\pi$	−0.96	−0.77	−0.62	−0.51	−0.43	−0.36	−0.30	−0.27
$2m(\delta_Z+\delta\mu_{N,\Delta}+\delta\mu_\pi)$	−0.65	−0.52	−0.42	−0.35	−0.29	−0.24	−0.20	−0.18
$2m\delta\mu_{\mathrm{c.m.}}$	−0.17	−0.15	−0.13	−0.12	−0.11	−0.10	−0.09	−0.09
$2m\mu_0$	−0.89	−1.01	−1.14	−1.26	−1.39	−1.52	−1.64	−1.77
$2m_\mu$	−1.71	−1.68	−1.69	−1.73	−1.79	−1.86	−1.94	−2.03
proton								
$\delta\langle r^2\rangle_Z$	−0.18	−0.17	−0.16	−0.15	−0.14	−0.13	−0.13	−0.12
$\delta\langle r^2\rangle_{N,\Delta}$	0.13	0.11	0.11	0.10	0.09	0.08	0.07	0.07
$\delta\langle r^2\rangle_\pi$	0.36	0.31	0.27	0.24	0.21	0.19	0.17	0.16
$\delta\langle r^2\rangle_Z+\delta\langle r^2\rangle_{N,\Delta}+\delta\langle r^2\rangle_\pi$	0.30	0.25	0.21	0.18	0.16	0.14	0.12	0.11
$\delta\langle r^2\rangle_{\mathrm{c.m.}}$	−0.08	−0.11	−0.14	−0.17	−0.21	−0.25	−0.29	−0.34
$\langle r^2\rangle_0$	0.25	0.33	0.42	0.52	0.62	0.74	0.87	1.01
$\langle r^2\rangle$	0.47	0.47	0.49	0.53	0.58	0.64	0.71	0.78
neutron								
$\delta\langle r^2\rangle_{N,\Delta}$	0.06	0.06	0.06	0.06	0.05	0.05	0.05	0.05
$\delta\langle r^2\rangle_\pi$	−0.36	−0.31	−0.27	−0.24	−0.21	−0.19	−0.17	−0.16
$\langle r^2\rangle_0$	0.00	0.00	0.00	0.00	0.00	0.00	0.00	0.00
$\langle r^2\rangle$	−0.30	−0.25	−0.21	−0.18	−0.16	−0.14	−0.12	−0.11

TABLE I. (*Continued.*)

$R_N(\mathrm{GeV}^{-1})$	3.5	4.0	4.5	5.0	5.5	6.0	6.5	7.0
δg_{AZ}	−0.80	−0.57	−0.42	−0.32	−0.25	−0.19	−0.15	−0.12
δg_{ANN}	0.06	0.04	0.03	0.02	0.02	0.02	0.01	0.01
$2\delta g_{AN\Delta}$	0.38	0.27	0.19	0.15	0.11	0.09	0.07	0.06
$\delta g_{A\Delta\Delta}$	0.15	0.10	0.07	0.05	0.04	0.03	0.02	0.02
$\delta g_{AZ}+\delta g_{ANN}+2\delta g_{AN\Delta}+\delta g_{A\Delta\Delta}$	−0.21	−0.16	−0.12	−0.09	−0.08	−0.06	−0.05	−0.04
$\delta g_{A\,\mathrm{c.m.}}$	0.42	0.32	0.25	0.21	0.17	0.14	0.12	0.11
g_A^0	1.09	1.09	1.09	1.09	1.09	1.09	1.09	1.09
g_A	1.30	1.26	1.22	1.20	1.18	1.17	1.16	1.16
$\delta\Gamma_Z/\Gamma^0$	−1.54	−1.06	−0.73	−0.50	−0.34	−0.20	−0.10	−0.02
$\delta\Gamma_{NN}/\Gamma^0$	0.91	0.69	0.53	0.41	0.30	0.23	0.16	0.12
$\delta\Gamma_{\Delta N}/\Gamma^0$	0.53	0.39	0.29	0.23	0.18	0.14	0.12	0.10
$\delta\Gamma_{N\Delta}/\Gamma^0$	0.05	0.04	0.03	0.02	0.02	0.02	0.01	0.01
$\delta\Gamma_{\Delta\Delta}/\Gamma^0$	0.27	0.19	0.14	0.10	0.08	0.06	0.04	0.04
$(\delta\Gamma_Z+\delta\Gamma_{NN}+\delta\Gamma_{\Delta N}+\delta\Gamma_{N\Delta}+\delta\Gamma_{\Delta\Delta})/\Gamma^0$	0.22	0.24	0.26	0.26	0.26	0.26	0.25	0.25
$\delta\Gamma_{\mathrm{c.m.}}/\Gamma^0$	1.16	0.89	0.70	0.57	0.46	0.40	0.34	0.28
Γ^0(MeV)	70	67	64	61	58	54	50	46
Γ(MeV)	166	143	126	112	100	89	80	71

$$D=(v'/v)^2-(v'/v)\frac{1}{k}-\frac{(v''/v)}{2}\,, \tag{3.16}$$

$$\delta\langle r^2\rangle_N=(\tfrac{3}{2}-\tfrac{1}{2}\tau_3)\frac{25}{9}\frac{1}{(2\pi)^2}\int\frac{k\,d\omega\,v^2(kR_N)}{\omega^2}\langle r_p{}^2\rangle_0\,, \tag{3.17}$$

$$\delta\langle r^2\rangle_\Delta=(1+\tfrac{5}{3}\tau_3)\frac{16}{3}\frac{1}{(2\pi)^2}\int\frac{k\,d\omega\,v^2(kR_N)}{(\omega_\Delta+\omega)^2}\langle r_p{}^2\rangle_0\,.$$

Here $v'=dv/dk$ and $v''=d^2v/dk^2$. The c.m. correction is obtained from (3.10) rather than using the method of Ref. 8. The dominant contribution arises from the wave-function overlap, which is more directly determined by computing the rms spread of the c.m. wave packet:

$$\left\langle\left(\frac{\vec{r}_1+\vec{r}_2+\vec{r}_3}{3}\right)^2\right\rangle=\tfrac{1}{3}\langle r_1{}^2\rangle=\tfrac{1}{3}\langle r_p{}^2\rangle_0\,. \tag{3.18}$$

Here $\vec{r}_i$ refers to the position of the ith quark, each of which appears in identical spherically symmetric orbitals. Since the charge density is used to give the quark distribution, the rms spread is proportional to the charge radius. From (3.10) the correction is

$$\delta\langle r^2\rangle=-(\tfrac{1}{2}+\tfrac{1}{2}\tau_3)\tfrac{1}{3}\langle r_p{}^2\rangle_0+O(1/m^2)\,. \tag{3.19}$$

The higher-order terms in $1/m^2$ are neglected.[16]

The corrected charge radii for the neutron and proton are given in Fig. 4 and Table I as a function of R.

D. Nucleon axial-vector charge

We consider here the order-$1/f^2$ renormalization of the axial-vector charge only, rather than the full axial-vector form factor. The relevant graphs for the axial-vector current are given in Fig. 3(c). The wave-function renormalization contributes

$$\delta g_Z=-g_A^0\epsilon_N\,. \tag{3.20}$$

The vertex renormalization from the four graphs of Fig. 3(c) is given in an obvious notation, respectively, by

$$\delta g_{NN}=g_A^0\frac{25}{27}\frac{1}{(2\pi)^2}\int\frac{k\,d\omega\,v^2(kR_N)}{\omega^2}\,, \tag{3.21}$$

$$\delta g_{\Delta N}=\delta g_{N\Delta}=g_A^0\frac{128}{27}\frac{1}{(2\pi)^2}\int\frac{k\,d\omega\,v^2(kR_N)}{\omega(\omega+\omega_\Delta)}\,, \tag{3.22}$$

$$\delta g_{\Delta\Delta}=g_A^0\frac{160}{27}\frac{1}{(2\pi)^2}\int\frac{k\,d\omega\,v^2(kR_N)}{(\omega_\Delta+\omega)^2}\,. \tag{3.23}$$

The c.m. correction is found by a procedure analogous to that described above (3.10) for the electromagnetic form factors.[13,16] The correction is

$$\delta g_{\mathrm{c.m.}}=g_A^0(\tfrac{1}{3}\langle p^2\rangle/m^2-\tfrac{5}{36}\langle p^4\rangle/m^4)\,. \tag{3.24}$$

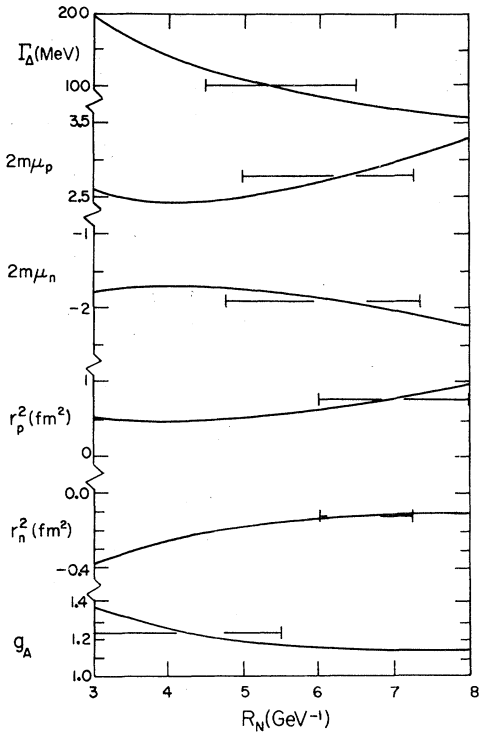

FIG. 4. Decay width of Δ (MeV), proton and neutron anomalous magnetic moment, proton and neutron squared charge radius (fm^2) and the nucleon axial-vector charge as a function of nucleon bag radius R_N (GeV^{-1}) calculated to order $1/f^2$ and adjusted for c.m. wave-packet size with $\bar{x}=2.043$.

The corrected value is plotted as a function of R_N in Fig. 4 and the various contributions are listed in Table I.

E. Decay width of the Δ(1232)

The decay width Γ_Δ of the Δ is of course proportional to the square of the $\pi N\Delta$ on-shell coupling constant $g^{\pi N\Delta}$. The contributions to this constant are analogous to those for the πNN coupling constant described above [see Fig. 3(d)]. They are

$$\delta g_Z^{\pi N\Delta} = -g_0^{\pi N\Delta}\left(\frac{\epsilon_N}{2}+\frac{\epsilon_\Delta}{2}\right), \tag{3.25}$$

$$\delta g_{NN}^{\pi N\Delta} = g_0^{\pi N\Delta}\,\frac{100}{27}\,\frac{1}{(2\pi)^2}\,P\int\frac{k\,d\omega\,v^2(kR_N)}{(\omega-\omega_\Delta)\omega}, \tag{3.26}$$

$$\delta g_{\Delta N}^{\pi N\Delta} = g_0^{\pi N\Delta}\,\frac{125}{27}\,\frac{1}{(2\pi)^2}\int\frac{k\,d\omega\,v^2(kR_N)}{\omega^2}, \tag{3.27}$$

$$\delta g_{N\Delta}^{\pi N\Delta} = g_0^{\pi N\Delta}\,\frac{8}{27}\,\frac{1}{(2\pi)^2}\,P\int\frac{k\,d\omega\,v^2(kR_N)}{(\omega_\Delta+\omega)(\omega-\omega_\Delta)}, \tag{3.28}$$

$$\delta g_{\Delta\Delta}^{\pi N\Delta} = g_0^{\pi N\Delta}\,\frac{100}{27}\,\frac{1}{(2\pi)^2}\int\frac{k\,d\omega\,v^2(kR_N)}{\omega(\omega_\Delta+\omega)}, \tag{3.29}$$

$$\delta g_{\text{c.m.}}^{\pi N\Delta} = g_0^{\pi N\Delta}(\langle p^2\rangle/2m^2 - \langle p^4\rangle/8m^4). \tag{3.30}$$

The results for Γ_Δ are given in Fig. 4 and Table I.

F. Discussion

For comparison with the experimentally measured quantities we use the values $2m_p\mu_p = 2.79$, $2m_n\mu_n = -1.91$, $\Gamma_\Delta = 103$ MeV,[17] $g_A = 1.24$,[18] $\langle r_p^2\rangle = -0.77\pm0.05$ fm^2, and $\langle r_n^2\rangle = -0.12\pm0.01$ fm^2.[19] In Fig. 4 the bars are drawn so as to intercept the central experimental values. They are extended to represent the allowed range of R_N due to the theoretical uncertainty in the determination of the various quantities. The quantities μ_p, μ_n, and g_A are assigned a theoretical uncertainty of ±10% and the quantities Γ_Δ, $\langle r_p^2\rangle$, and $\langle r_n^2\rangle$, ±20%, since they are squared relative to the others. The measure of uncertainty in the c.m. correction is the ratio of the kinetic energy to the total energy,

$$\langle p^2\rangle/2m^2 = 3(\bar{x}/mR)^2/2. \tag{3.31}$$

The next-higher terms are given in (3.12), (3.24), and (3.30). Although more information about $\phi(p)$ (3.8) is needed to calculate these terms, it is clear that including them will decrease the magnitude of the magnetic moments, thereby requiring somewhat larger values of R_N, and decrease g_A and Γ_Δ, thereby requiring somewhat smaller values of R_N. This higher-order correction to g_A is sufficiently large at small R_N that one cannot reliably distinguish theory from experiment in this range. For this reason the bar for g_A is extended indefinitely to low values of R_N. For that matter, one could claim such a great theoretical uncertainty that all values are consistent with experiment for $R_N \lesssim 3.5$ GeV^{-1}. The measure of uncertainty due to terms of higher order in the pion coupling is

$$\epsilon = \left(\frac{g_A}{2\pi f R_N}\right)^2, \tag{3.32}$$

slightly different from Jaffe's measure.[20] It is generally smaller than the uncertainty in the c.m. correction. For larger values of R_N the largest uncertainty probably arises from the idealization of the hadron boundary as a sharp surface. These considerations entered into the estimate of a 10% theoretical error. In addition the model has ignored the effect of quark correlations induced by the gluon interaction. The latter effect has been used by some authors to account entirely for the nucleon charge radii without any provision for a pion field.[21] If the effect discussed by these authors is found in the bag model, it would increase $\langle r_p^2\rangle$, a desirable result, but increase the

magnitude of $\langle r_n^2 \rangle$, an undesirable result.

Clearly there is no particular nucleon radius for which all parameters agree with the experimental values within the assigned theoretical uncertainties. However, agreement is worse for $R_N \leq 4$ GeV^{-1}. Thus, barring any surprises from higher-order pion corrections, these results cast doubt on small-radius versions of the nucleon.[4] From Fig. 4 we find that the range $4.5 < R_N < 5.5$ GeV^{-1} gives approximate agreement for the magnetic moments, Γ_Δ and g_A. In this range the proton squared charge radius is in the range 0.49 to 0.71 fm^2, at most 35% low, and the neutron squared charge radius is in the range -0.21 to -0.12 fm^2, too large at worst by 75%. These quantities are particularly sensitive to the treatment of the bag surface and the neglect of correlations among the quarks; therefore we do not weight them as much in choosing the preferred range. In the range $4.5 < R_N$ 5.5 GeV^{-1} the error in the c.m. correction is estimated from (3.31) to be about 25% of the value of the correction. Thus the quantity of largest uncertainty is Γ_Δ with an error of 15% of its net value from this source, the expected error in other quantities being about 10%. The error in the pion renormalization, estimated from (3.32), is about 20% of the change due to renormalization, or less than 10% of the value of all quantities except $\langle r_n^2 \rangle$ for which it is 20%. The approximate equality of both errors justifies the neglect to this order of c.m. corrections to the pion corrections.

Increasing $\bar{x}$ by 20% has the effect of increasing the magnitudes of all quantities except the charge radii. Agreement with experiment occurs at higher R_N for Γ_Δ and g_A and lower R_N for μ_p and μ_n, giving slightly better concurrence of the results (see IV C below).

IV. BAG-MASS RENORMALIZATION

A. Unrenormalized mass

For the unrenormalized masses, we use the model of Johnson,[3] which includes an approximation to the original model[2] as a special case. In this version of the bag model the cavity energy for a bag with n massless quarks in the $S_{1/2}$ orbital is given by

$$E_0 = n\frac{2.04}{R} + \frac{Z(R)}{R} + \mu\frac{\alpha_S(R)}{R} + \frac{4\pi}{3}BR^3 , \tag{4.1}$$

where the terms are, respectively, the quark kinetic energy, the zero-point energy, the gluon interaction energy with $\mu_\pi = -0.70$, $\mu_{\rho,\omega} = 0.70/3$, $\mu_N = -0.70/2$, $\mu_\Delta = 0.70/2$, and the bag volume energy. The mass is found by correcting for the c.m. motion, thus

$$M^2 = E^2 - n(\bar{x}/R^2) , \tag{4.2}$$

where $\bar{x} \approx 2$. Johnson uses a scale-dependent coupling constant

$$\alpha_S(R) = \frac{2\pi}{9\ln(\kappa + 1/R\Lambda)} \tag{4.3}$$

and chooses $\kappa = 1$. This form is not derived. It is introduced in order to give smooth behavior for $R\Lambda \approx 1$ and the correct lowest-order scaling for $R\Lambda \ll 1$.[22] A novel feature of Johnson's version of the bag model is the form of the zero-point energy, proportional to

$$Z(R) = a - b\alpha(R) . \tag{4.4}$$

The constant a represents the finite Casimir effect to lowest order in $\alpha(R)$, which has been calculated, but remains controversial because of uncertainties in the physical relevance of the high-frequency modes.[2,23] Values of 0.30 to 0.65 have been quoted for a. The second term represents second-order vacuum fluctuations that also contribute to the Casimir effect. They have not been calculated. Johnson argues that they are attractive and treats b as an adjustable, positive constant.

A principal innovation of Johnson's scheme is his model for the quantum-chromodynamics (QCD) vacuum that pictures it as a dense static ensemble of empty bags. The bag constant is the energy density of such a vacuum, relative to the zero-field vacuum so that

$$-B = \frac{1}{\frac{4}{3}\pi R_0^4}[a - \alpha(R_0)b] , \tag{4.5}$$

where R_0 is the radius for which $-B$ is minimized. It is assumed that the vacuum is completely saturated. This constraint reduces the number of free parameters, giving $B^{1/4}/\Lambda$ as a function of a, b, and κ (4.3). We may on occasion consider parameter values that do not satisfy (4.5). Without (4.5) the original model[2] can be recovered in the approximation Λ large, $b = 0$ so that α depends only on κ and Z only on a. The c.m. momentum correction can be kept in the form (4.2) or absorbed into Z with the choice $\bar{x} = 0$ as in the approximation of the original model.[8]

B. Renormalization of bag masses

1. *Nucleon and Δ(1232)*

Prior to the advent of the quark model, Chew and Low proposed a model for the Δ based on a cutoff Yukawa theory for low-energy pion-nucleon interactions.[10] The Chew-Low model differs from the present model in that the bare Δ is absent and the form factor $v(kR)$ is replaced by a cutoff P-

wave phase-space factor, appropriate to a pointlike nucleon (i.e., $R \to 0$). The model produced the Δ as a πN resonance when the cutoff was set at $k \approx 1$ GeV. The bag form factor $v(kR)$ for $R \approx 5$ GeV^{-1} is so much weaker than the pointlike form factor of the Chew-Low model that no Δ-like resonance is produced in the absense of an explicit bare Δ.[6] Thus the bare Δ in the bag model plays the role of a Castillejo-Dalitz-Dyson pole[24] in the Chew-Low equation rather than a pole arising directly from the πN interaction. Accordingly, we shall consider the Δ and N in perturbation theory starting from the bag states. The lowest-order self-energies of Fig. 3(a) are modified by the contributions of Fig. 5. Summing these self-energies to all orders, but neglecting intermediate states with more than two pions corresponds closely to the Chew-Low model with an additional elementary Δ. Because of the weakness of the form factor, the higher-order graphs of Fig. 5 and others give a negligible contribution to the real part of the mass shift, and give a small but more significant contribution to the imaginary part.[25] Thus the real part of the mass shift is given to a good approximation by (3.1) and the imaginary part of the mass shift of the Δ is found to a good approximation by the method of Sec. III E, which is equivalent to computing the imaginary part of the self-energy diagrams of Fig. 5, together with those of Fig. 3(a), but in the latter diagrams, using the unrenormalized coupling constants.

2. *The mesons* ρ, ω, *and* π

The static model is applied with much less certainty to the lighter hadrons. We consider only the lowest-order self-energies here, given in Fig. 6. The degenerate static limit is a reasonable approximation for the ω. For a massless pion, a generalization of expression (2.18) of I applies, namely,

$$\Delta E = -\frac{9}{100}\frac{g_A^2}{8\pi f^2 R_\omega^3}\left\langle \sum_{i,j} \epsilon_i \vec{\sigma}_i \vec{\tau}_i \cdot \epsilon_j \vec{\sigma}_j \vec{\tau}_j \right\rangle, \qquad (4.6)$$

where we must use $\epsilon = +1$ for quarks and -1 for antiquarks. In the case of the ω meson, the only intermediate state in the decomposition

$$\sum_\lambda \left\langle \omega \left| \sum_i \epsilon_i \vec{\sigma}_i \vec{\tau}_i \right| \lambda \right\rangle \left\langle \lambda \left| \sum_j \epsilon_j \vec{\sigma}_j \vec{\tau}_j \right| \omega \right\rangle \qquad (4.7)$$

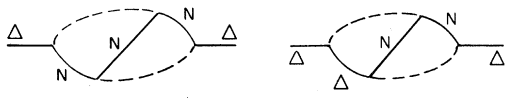

FIG. 5. Example of diagrams contributing to the Δ self-energy to order $1/f^4$.

TABLE II. Contribution to $\langle \sum_{i,j} \vec{\sigma}_i \vec{\tau}_i \cdot \vec{\sigma}_j \vec{\tau}_j \rangle$ from the various intermediate states.

N	25 (N)	32 (Δ)
Δ	8 (N)	25 (Δ)
ρ	8 (ω)	8 (π)
ω	24 (ρ)	
π	24 (ρ)	

is the ρ meson (neglecting quark excitations), and the expectation value is 24 (see Table II). If we convert to momentum space and give the pion a physical mass, (4.6) becomes

$$\Sigma_\omega(m_\omega) = -\frac{1}{(2\pi)^2}\frac{24}{3}\int_{m_\pi}^{\infty} \frac{k\,d\omega\, v^2(kR_\omega)}{\omega}, \qquad (4.8)$$

which may also be derived directly from momentum-space matrix elements as was done for N and Δ [see (2.3) and (3.1)].

For the ρ meson the spin-isospin factor is decomposed into π and ω contributions as shown in Fig. 6 and Table II. The ω contribution is treated as above giving exactly $\frac{1}{3}$ the mass shift (4.8). The π contribution, however, must be handled differently. The ρ_{bag}-π_{bag}-π_{field} vertex is calculated with degenerate ρ and π bag states, but we wish to use the physical mass for the pion. The recoil of the π bag state is neglected, but a relativistic treatment is obviously more appropriate. In addition the π_{bag} and π_{field} states are in fact identical, so one must avoid double counting the intermediate state. We propose using the vertex calculated for the degenerate case as the physical form factor, with the momentum k representing the c.m. momentum of the intermediate pion and with no correction for the continuation to the physical pion mass. These assumptions are embodied in the $\rho\pi\pi$ vertex function

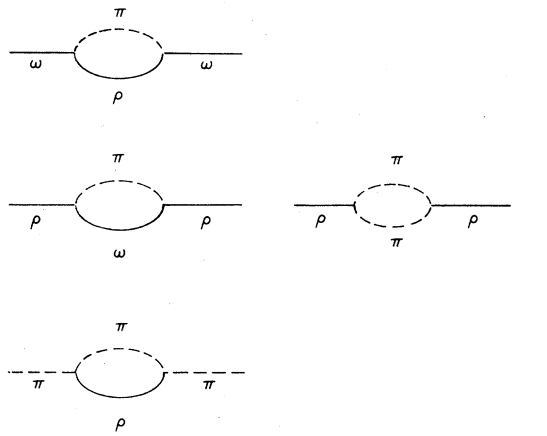

FIG. 6. Contribution to meson self-energies to order $1/f^2$.

$$-i\epsilon_{ijk}(2k-p)_\mu \frac{v(|\vec{k}|R_\rho)}{|\vec{k}|}\sqrt{2m_\rho}\,, \tag{4.9}$$

where i refers to the Cartesian isospin index of the ρ, j, and k to pions, p is the four-momentum of the ρ meson, and k, that of the pion. The quantity $|\vec{k}|$ is evaluated in the c.m. of the ρ meson. The mass shift for the ρ meson becomes

$$\Sigma_\rho(m_\rho) = -\frac{1}{(2\pi)^2}\frac{8}{3}\int_{m_\pi}^{\infty}\frac{k\,d\omega\,v^2(kR_\rho)}{\omega} + \frac{1}{(2\pi)^2}\frac{8}{3}\int_{m_\pi}^{\infty} k\,d\omega\,v^2(kR)\frac{2m_\rho}{m_\rho^2-4\omega^2+i\epsilon}\,. \tag{4.10}$$

The two terms arise from the $\omega\pi$ and $\pi\pi$ intermediate states, respectively. The second term has been reduced by $\frac{1}{2}$ to correct for double counting. The decay width of the ρ meson is then

$$\Gamma_\rho = \frac{2}{3\pi}k_\rho v^2(k_\rho R)\,. \tag{4.11}$$

Because of the approximations involved in (4.10), the mass of the ρ cannot be computed as reliably as that of the N, Δ, or ω.

The mass of the π meson is also renormalized through the process shown in Fig. 6. We have used

$$\Sigma_\pi(m_\pi)\approx\frac{1}{(2\pi)^2}\frac{24}{3}\int k\,d\omega\,v^2(kR_\pi)\left(\frac{1}{m_\pi-m_\rho^2/2m_\pi-\omega}+\frac{\omega}{\omega'}\frac{m_\pi}{2m_\pi\omega'+m_\rho^2}\right), \tag{4.12}$$

where $\omega' = (k^2+m_\rho^2)^{1/2}$. This form is based on the vertex (4.9) but with a form factor that reflects the size of the pion. The ambiguities in a continuation from the SU(6) degenerate mass to the physical mass make this result rather unreliable.

C. Adjustment of parameters

There are six parameters Λ, a, b, κ, $\bar{x}$, and B to be adjusted to produce five masses m_Δ, m_N, m_ρ, m_ω, and m_π and a nucleon radius in a range such that the several parameters of Fig. 4 are close to the experimental values. In addition we may want to consider following Johnson[3] and impose the constraint (4.5). Although there are correlations among the masses, particularly m_ρ and m_ω, there are also correlations among the parameters; the net effect as it turns out is to overconstrain the parameters. Therefore, we seek solutions giving preference to the nucleon, Δ, and ω masses and the parameters of Sec. III in this order.

The masses are calculated following the procedure discussed in I. After minimizing $E_0(R)$ (4.1) at $R=R_0$ for a given hadron, we evaluate

$$E(R_0) = E_0(R_0) + \Sigma(R_0)\,, \tag{4.13}$$

and then apply the correction (4.2) at the value R_0. Thus we are treating the pion self-energy and the c.m. correction as independent perturbations of comparable order. The shift in R_0 to order $1/f^2$ is determined from I to be

$$\delta R = -\Sigma'(R_0)/E_0''(R_0)\,, \tag{4.14}$$

where, using (4.1) and $E_0'(R_0)=0$,

$$E_0''(R_0) = 16\pi B R_0 + (\mu-b)\alpha_s''(R_0)/R_0\,. \tag{4.15}$$

It is found that the best results are obtained in the limit of large Λ without the constraint (4.5)—i.e., using the original version of the model[1] but with a c.m. correction given by (4.2).[26] The values of the masses, radii, and coupling constants are shown in Table III. The pion mass is somewhat large. Thus we are unable to produce the zero-mass pion of Donoghue and Johnson without further modification of the model.[8] However, the computation of the pion self-energy Σ_π is sufficiently unreliable that we do not consider this to be a serious defect of our calculation. The shift in nucleon radius $\delta R_N = -0.5$ GeV^{-1} results in a net radius of $R_N = 4.5$ GeV^{-1}, the lowest radius preferred by the various nucleon parameters of Fig. 4.

For comparison, we have also considered using the currently conventional method which minimizes $M^2(R)$ (4.2). In this case the perturbed bag masses are given by first minimizing the unperturbed mass formula to determine R_0 and then evaluating (4.2) at R_0, but with $E(R_0)=E_0(R_0)+\Sigma(R_0)$. The order-$1/f^2$ shift in radius is found in analogy with (4.14) to be

$$R = R_0 - [2E_0(R)\Sigma(R)]'/M^{2\prime\prime}(R)\big|_{R=R_0}\,. \tag{4.16}$$

The best results are shown in Table IV. In this

TABLE III. Results of calculation with correction for c.m. motion applied after minimization of the bag energy.

	m (MeV)	R_0 (GeV^{-1})	δR(GeV^{-1})	Σ (MeV)	α_s
N	942	5.1	−0.6	−142	1.6
Δ	1235	5.4	−0.5	−126	1.6
ρ	836	4.8	−0.2	−56	1.6
ω	787	4.8	−0.2	−95	1.6
π	268	4.3	−0.1	−33	1.6

$\bar{x}=2.04$, $\kappa=1.52$, $a=-0.55$, $b=0$

$B^{1/4}/\Lambda=0.020$, $\Lambda=7788$ MeV, $B^{1/4}=156$ MeV

$\Gamma_\rho=86$ MeV

TABLE IV. Results of calculation with minimization of the bag mass after correction for c.m. motion.

	m (MeV)	R_0 (GeV^{-1})	δR (GeV^{-1})	Σ (MeV)	α_s
N	938	4.9	−1.0	−167	1.6
Δ	1229	5.0	−0.8	−156	1.6
ρ	834	4.3	−0.7	−81	1.4
ω	769	4.3	−1.0	−132	1.4
π	396	3.8	−0.4	−45	1.3

$\bar{x}=2.04$, $\kappa=1$, $a=0.4$, $b=0.52$

$B^{1/4}/\Lambda=0.42$, $\Lambda=375$ MeV, $B^{1/4}=158$ MeV
$\Gamma_\rho=97$ MeV

example we have used Johnson's constraint. The shift in nucleon radius is substantial, giving a net $R_N=3.9$ GeV^{-1}, reflecting the destabilizing effect of this procedure for treating the c.m. correction. For this reason we prefer the former method.

To illustrate the sensitivity to the choice of parameters, we give results of an alternative calculation in Table V, once again minimizing $E(R)$ before correcting for c.m. motion. Here we use $\bar{x}=2.5$ and obtain a slightly larger nucleon and more massive pion. This parametrization respects the constraint (4.5).

The width of the ρ meson was calculated using (4.11) without c.m. corrections or higher-order corrections in $1/f^2$. It is lower than the experimental value ($\Gamma_\rho=158$ MeV) (Ref. 17) as was the bare value of Γ_Δ.

Although the pion mass is rather large in all three examples it should be noted that the c.m. correction (4.2) for the pion is substantial. In the example of Table III, the bag energy before correction is 730 MeV and the c.m. momentum is 680 MeV. Therefore, it would take only a 7% decrease in bag energy to reduce the mass to zero. The corresponding decrease for Table IV is 12% and for Table V, 10%. It is quite likely that these figures are within the margin of error of the model. Nevertheless, one may be surprised that it was not possible by a slight change in parameters to produce a zero-mass pion as did Donoghue and Johnson.[3,8] The reason lies in the following peculiarity of the calculation: The nucleon mass arises from a positive bag contribution that is essentially proportional to a scale parameter, say $B^{1/4}$, and a negative self-energy due to the pion cloud that has an intrinsic scale set by the pion decay constant f and grows violently as the radius shrinks. The optimum mass, as a function of this scale, is dominated at small B (large radii) by the bag contribution, and at large B by the pion self-energy. Thus there is a maximum value of the optimum mass that usually occurs at uncorrected radii of 4 to 4.5 GeV^{-1}. If this maximum is smaller than 940 MeV, the correct nucleon mass cannot be reached. The excluded portion of parameter space is the part that includes zero-mass pions. At the edge of the excluded portion the corrected nucleon radius is too small to give reasonable values for the nucleon parameters of Fig. 4. If the strong-coupling constant is scale dependent with a small value of Λ, the ρ-π mass splitting is reduced (these being of smaller radius), giving a higher pion mass. For this reason large values of Λ are preferred. Increasing $\bar{x}$ does not help, as we see from Table V. The reason for this is that in doing so, the proton mass is reduced, requiring a shift in the other parameters, and enlarging the excluded region of parameter space.

TABLE V. Calculation with $\bar{x}=2.5$ using the procedure of Table III.

	m (MeV)	R_0 (GeV^{-1})	δR (GeV^{-1})	Σ (MeV)	α_s
N	939	5.2	−0.5	−138	1.7
Δ	1230	5.2	−0.5	−138	1.7
ρ	824	4.7	−0.1	−59	1.5
ω	770	4.7	−0.2	−99	1.5
π	355	4.6	−0.0	−27	1.5

$\bar{x}=2.5$, $\kappa=1$, $a=0.3$, $b=0.42$

$B^{1/4}/\Lambda=0.435$, $\Lambda=372$ MeV, $B^{1/4}=162$ MeV
$\Gamma_\rho=87$ MeV

It is interesting to compare the parametrization of Tables III–V with those of the original model.[2] Because of the large value of Λ, the strong coupling constant in Table III is essentially independent of R, and is about 25% smaller than that of Ref. 2.[27] The principal reason for this reduction is that the pion self-energy shifts the baryon masses by more than the meson masses. In the original version of the model such a shift is compensated by a larger value of Z_0 and a smaller value of α_s. The pion self-energy by itself does not contribute significantly to the N-Δ mass splitting.

With the larger value of $\bar{x}$ of Table V it is necessary to recompute the parameters of Table I that have $\bar{x}$-dependent c.m. corrections. The new values are given in Table VI. The charge radii are the same as in Table I. If the same criterion for theoretical error is applied here as in Fig. 4 and Sec. III, then any value of R_N in the range 3.5 to 7 GeV^{-1} gives acceptable nucleon magnetic moments, values from 4.5 to 8.0 give acceptable values of g_A, but the results for Γ_Δ suggest $5.0 \leq R_N \leq 7.0$. Thus considering the charge radii as well, complete harmony occurs in the range $R_N=6$–7

TABLE VI. Baryon parameters with $\bar{x}=2.5$.

	3.0	3.5	4.0	4.5	5.0	5.5	6.0	6.5	7.0	7.5	8.0
$2m_p\mu_p$	2.89	2.74	2.70	2.70	2.72	2.78	2.87	2.98	3.11	3.24	3.39
$2m_n\mu_n$	−1.79	−1.76	−1.76	−1.76	−1.79	−1.84	−1.91	−1.99	−2.07	−2.17	−2.26
g_A	1.51	1.42	1.42	1.35	1.30	1.27	1.24	1.22	1.21	1.19	1.18
Γ_Δ (MeV)	207	173	173	148	129	113	100	88	78	69	60

GeV^{-1}. However, the hadron masses cannot be reproduced at this radius. On the other hand, at $R_N=4.7$ GeV^{-1}, as suggested by Table V, the results are as good as those of Table III with $\bar{x}=2.04$. Therefore, we consider either parametrization to be acceptable, although that of Table III gives a somewhat better pion mass.

Finally, we illustrate the sensitivity of the parameter adjustment to the assumption that the size of the pion and a finite spread of the bag surface can be neglected. If the bag radius R is regarded as the rms position of the bag surface, then an appreciable pion-bag interaction may instead occur at a separation $R'=(R^2+R_\pi^2)^{1/2}$. Replacing R in $v(kR)$ in Eq. (2.8) by R' has the effect of reducing the pion-field contribution substantially. The result of a calculation yielding a nearly zero-mass pion is summarized in Table VII. A nucleon radius of 5.1 GeV^{-1} is obtained, giving these values of the nucleon parameters: $2m\mu_p=2.82$, $2m\mu_n=-1.69$, $\langle r^2\rangle_p=0.49$ fm^2, $\langle r^2\rangle_n=-0.14$ fm^2, $g_A=1.40$, and $\Gamma_\Delta=103$ MeV. With the exception of a very low decay width of the ρ meson, the results are as satisfactory as those of Table III, but the modification in the model is rather *ad hoc*.

V. CONCLUSION AND DISCUSSION

Having incorporated the pion into the bag model and considered the effect of the finite size of the wave packet on the various static parameters, we find, on the whole, better agreement with measured masses and other parameters than in the original bag-model calculation without renormalization due to pion interactions. With the results of Table III and $R_N=4.5$ GeV^{-1}, we find (see Table I) $2m\mu_p=2.43$, $2m\mu_n=-1.69$, $g_A=1.22$, and $\Gamma_\Delta=126$ MeV, compared to previous values of 2, −1.3, 1.09, and 50 MeV, respectively.[2,11] The calculated squared charge radius of the proton, 0.49 fm^2 has not improved, but the neutron has acquired a negative squared radius of roughly the correct magnitude. However, these latter parameters are strongly affected by quark correlations.[21]

The c.m. corrections are generally substantial and larger than the renormalization due to pion exchange. Thus it would seem that in order $1/f^2$ we have reached the limits of accuracy of the calculation. Further improvements must be sought in a better understanding of the origins of confinement. Such an understanding could provide a better description of the bag surface and a better characterization of the pion. Indirectly, it would provide a more accurate c.m. wave function.

Within the more limited scope of the present calculation one may want to study further the effect of incorporating explicitly quark-antiquark pairs in place of the internal pion field, as discussed in I. The effect of the internal field upon the calculation is substantial. Without the internal field, the value of g_A would be 50% larger[22] and Γ_Δ would be more than twice as large. In our calculation it is not possible to accommodate such values.

Finally, there is the question of the size of the nucleon bag.[4] Although we are unable to study the regime $R_N<3.5$ GeV^{-1} because the perturbation theory fails, we find that reasonably good results for several baryon parameters and hadron masses can be obtained with $R_N\approx 4.5$ GeV^{-1}. At this radius the expansion parameter for c.m. corrections is $\langle p^2\rangle/2m^2\approx 0.3$ and for pion corrections, $\epsilon\approx 0.2$ [see (3.32)]. Therefore, the use of perturbation theory is justified *a posteriori*.

TABLE VII. Calculation illustrating the possible effect of a finite pion size, otherwise using the procedure of Table III.

	m (MeV)	R_0 (GeV^{-1})	δR (GeV^{-1})	Σ (MeV)	α_s
N	940	5.2	−0.09	−27	1.7
Δ	1236	5.2	−0.10	−20	1.7
ρ	781	4.8	−0.04	−8	1.6
ω	748	4.8	−0.03	−30	1.6
π	17	4.7	−0.02	−10	1.5

$\bar{x}=2.7$, $\kappa=1$, $a=0.65$, $b=0.8$

$B^{1/4}/\Lambda=0.440$, $\Lambda=370$ MeV, $B^{1/4}=163$ MeV

$\Gamma_\rho=44$ MeV

ACKNOWLEDGMENTS

I wish to thank Kenneth Johnson and John Donoghue for helpful discussions and Gerald Miller for a discussion of the results of Ref. 7 prior to the appearance of the report. This work was supported in part by a grant from the National Science Foundation.

[1]C. DeTar, preceding paper, Phys. Rev. D 24, 752 (1981).
[2]T. DeGrand, R. L. Jaffe, K. Johnson, and J. Kiskis, Phys. Rev. D 12, 2060 (1975).
[3]K. Johnson, in *Particles and Fields—1979*, proceedings of the Annual Meeting of the Division of Particles and Fields of APS, Montreal, edited by B. Margolis and D. G. Stairs (AIP, New York, 1980).
[4]G. E. Brown and M. Rho, Phys. Lett. 82B, 177 (1979); G. E. Brown, M. Rho, and V. Vento, *ibid.* 84B, 383 (1979); V. Vento, M. Rho, E. M. Nyman, J. H. Jun, and G. E. Brown, Nucl. Phys. A345, 413 (1980).
[5]M. Barnhill, K. Cheng, and A. Halprin, Phys. Rev. D 20, 727 (1979); M. V. Barnhill and A. Halprin, *ibid.* 21, 1916 (1980).
[6]G. A. Miller, A. W. Thomas, and S. Théberge, Phys. Lett. 91B, 192 (1980); S. Théberge, A. W. Thomas, and G. A. Miller, Phys. Rev. D 22, 2838 (1980).
[7]Miller, Thomas, and Théberge in independent work have carried out a comprehensive analysis similar to ours, but emphasizing excellent agreement with the πN P_{33} phase-shift data in a static Chew-Low–type model. Their model for the quark bag is slightly different from ours, and they do not consider the effect of corrections for c.m. motion nor the chiral nonlinear boundary condition as we do. G. A. Miller, A. W. Thomas, and S. Théberge, University of Washington, Seattle report, 1980 (unpublished).
[8]J. Donoghue and K. Johnson, Phys. Rev. D 21, 1975 (1980); K. Johnson, in *High Energy Physics in the Einstein Centennial Year*, proceedings of Orbis Scientiae 1979, Coral Gables, edited by A. Perlmutter, F. Krausz, and L. F. Scott (Plenum, New York, 1979), p. 191.
[9]C. DeTar, in *Quantum Flavordynamics, Quantum Chromodynamics and Unified Theories*, edited by K. T. Mahanthappa and James Randa (Plenum, New York, 1979), p. 439 ff.
[10]G. Chew and F. Low, Phys. Rev. 101, 1570 (1956).
[11]A. Chodos and C. B. Thorn, Phys. Rev. D 12, 2733 (1975).
[12]In this work we do not consider taking into account the finite size of the pion, which would increase the form-factor radius. (But see the discussion of Table VII in Sec. IV.)
[13]W. Pauli, *Meson Theory of Nuclear Forces* (Interscience, New York, 1946).
[14]G. T. Adylov *et al.*, Phys. Lett. 51B, 402 (1975).
[15]These are normalized as usual, according to $\bar{u}u = 1$. We are using $G_E = F_1 + F_2$ and $G_M = F_1$ here.
[16]It is amusing that if we assume a Gaussian c.m. wave function, this spatial spread in the wave packet is consistent with the momentum spread of (3.13), provided $\bar{x} = 2.06$.
[17]Particle Data Group, Rev. Mod. Phys. 52, S1 (1980). For Γ_Δ we use the position of the pole.
[18]P. A. Schreiner, in *Neutrinos—1974*, proceedings of the Fourth International Conference on Neutrino Physics and Astrophysics, Philadelphia, edited by C. Baltay (AIP, New York, 1974), p. 101.
[19]R. W. Berard *et al.*, Phys. Lett. 47B, 355 (1973); V. E. Krohn and G. R. Ringo, Phys. Rev. D 8, 1305 (1973); F. Borkowski *et al.*, Nucl. Phys. A222, 269 (1975).
[20]R. J. Jaffe, in Proceedings of the 1979 Summer School "Ettore Majorana" on Subnuclear Physics (unpublished).
[21]R. Carlitz, S. D. Ellis, and R. Savit, Phys. Lett. 68B, 443 (1976); N. Isgur, Acta Phys. Pol. B8, 1081 (1977); N. Isgur, Phys. Rev. Lett. 41, 1269 (1978).
[22]H. D. Politzer, Phys. Rep. 14C, 129 (1974); D. J. Gross and F. A. Wilczek, Phys. Rev. Lett. 30, 1343 (1973); H. D. Politzer, *ibid.* 30, 1346 (1973).
[23]T. H. Boyer, Phys. Rev. 174, 1764 (1968); R. Balian and B. Duplantier, Ann. Phys. (N.Y.) 112, 165 (1978); K. A. Milton, L. L. DeRaad, and J. Schwinger, *ibid.* 115, 388 (1978); Kimball A. Milton, Phys. Rev. D 22, 1441 (1980); 22, 1444 (1980).
[24]L. Castillejo, R. H. Dalitz, and F. H. Dyson, Phys. Rev. 101, 453 (1956).
[25]For $R_N = 5$ GeV^{-1} we find that the order $1/f^4$ corrections shift the real part of m_N and m_Δ by about -15 MeV.
[26]Almost identical results may be obtained with the constraint by using a small, positive value of a and a nonzero value of b. However, a large value of Λ gives very small empty bags, contrary to the spirit of Johnson's model, so we see no reason to use the constraint here.
[27]The QCD coupling constant α_s is to be compared with $4\alpha_c$ of Ref. 2.